

Theoretical investigation of the parametric X-ray features

I.D. Feranchuk, A.V. Ivashin

► **To cite this version:**

I.D. Feranchuk, A.V. Ivashin. Theoretical investigation of the parametric X-ray features. Journal de Physique, 1985, 46 (11), pp.1981-1986. <10.1051/jphys:0198500460110198100>. <jpa-00210147>

HAL Id: jpa-00210147

<https://hal.archives-ouvertes.fr/jpa-00210147>

Submitted on 1 Jan 1985

HAL is a multi-disciplinary open access archive for the deposit and dissemination of scientific research documents, whether they are published or not. The documents may come from teaching and research institutions in France or abroad, or from public or private research centers.

L'archive ouverte pluridisciplinaire **HAL**, est destinée au dépôt et à la diffusion de documents scientifiques de niveau recherche, publiés ou non, émanant des établissements d'enseignement et de recherche français ou étrangers, des laboratoires publics ou privés.

Classification
 Physics Abstracts
 07.85 — 29.90

Theoretical investigation of the parametric X-ray features

I. D. Feranchuk and A. V. Ivashin

Department of Physics, Byelorussian State University, Minsk-80, U.S.S.R.

(Reçu le 29 janvier 1985, accepté sous forme définitive le 11 juillet 1985)

Résumé. — Dans cet article on présente les calculs numériques de la distribution spectrale et angulaire des rayons X paramétriques pour différents cristaux. On analyse leurs variations en fonction de l'énergie des particules.

Abstract. — The numerical calculation of the parametric X-ray spectral and angular distributions for different crystals is performed. Their dependence on the particle energy is discussed.

1. Parametric X-rays (PX) are one of several radiation types which originate when a relativistic charged particle interacts with a crystal. A review of the articles where PX have been considered and the detailed theory of this phenomenon are presented in paper [1]. The comparative analysis of various X-ray sources has shown that PX give the highest spectral intensity in comparison with other radiation mechanisms [2].

In the present paper we have calculated the spectral and angular distributions of PX for three specific crystals and for different values of the particle energy. These results are essential in order to choose the optimum conditions for the experimental investigation of PX.

2. In accordance with reference [1], the condition for PX is satisfied by the fact that the photon refraction index $n(\mathbf{\kappa}, \omega)$ is more than unity when the Bragg condition is fulfilled

$$(\mathbf{\kappa} + \boldsymbol{\tau})^2 \simeq \kappa^2, \quad (1)$$

where $\boldsymbol{\tau}$ is the reciprocal lattice vector, $\mathbf{\kappa}$ is the wave vector of the emitted photon, and ω is its frequency.

As a result, the condition of the Vavilov-Cherenkov radiation [3] ($\hbar = c = 1$)

$$1 - vn(\mathbf{\kappa}, \omega) \cos \theta = 0 \quad (2)$$

is satisfied in the crystal, in contrast with the homogeneous medium, where $n < 1$ for X-rays [4]. Here v is the charged particle velocity and θ is the angle between the vectors \mathbf{v} and $\boldsymbol{\tau}$. Thus, the Vavilov-Cherenkov radiation under the diffraction condition (1) is the parametric X-rays.

It has been shown [1] that one can obtain a qualitative description of PX by considering the diffraction by the crystal of pseudophotons [1], forming the relativistic charged particle electromagnetic field. Therefore PX give the same reflections as those formed when an X-ray beam with angular spread $\Delta\theta \sim m/E$ is diffracted by the crystal [1] (m is the mass of the particle and E is its energy). Consequently, PX as well as X-ray diffraction can be considered in two cases : 1) dynamic theory and 2) kinematic theory. The first case is realized in ideal crystals of thickness L , greater than the X-ray extinction length. In this case, PX reflections contain the most detailed information about the crystal structure.

On the other hand, the kinematic theory of PX is applicable for real crystals, which consist of thin mosaic blocks turned relative to each other at the angle $\delta > m/E$ [5]. This case is also realized for the particle beam with angular spread $\Delta\psi > m/E$ [5]. The kinematic diffraction is more convenient for the experimental observation of PX and it can be most easily analysed because the angular and spectral distributions of PX are essentially simplified and have a universal form for different crystals. Therefore we shall only consider this case.

The formula for the number of photons emitted by a charged particle in a thin crystal with $\kappa L |n-1| < 1$ was first obtained by Ter-Mikaeljan [6]. He treated the interaction between the crystal and photons as a perturbation. It was shown in [5] that PX from different blocks are incoherent and that the results [6] remain correct in the mosaic crystal with $\delta > m/E$ under the condition that one takes into account the refraction of photons and the multiple scattering of

electrons in the crystal. Then the spectral and angular distributions of emitted photons are defined by the simple expression which follows from the general formula (18) (see [1])

$$\frac{\partial^2 N}{\partial \mathbf{n}_\perp \partial \omega} = \frac{e^2}{2\pi} \omega L_a |g_\tau|^2 \frac{|\mathbf{K}_\perp, \omega \mathbf{v} + \boldsymbol{\tau}|^2}{\left[(\mathbf{K}_\perp - \boldsymbol{\tau}_\perp)^2 + \frac{\omega^2}{v^2} (1 - v^2) \right]^2} \left[1 - \exp\left(-\frac{L}{L_a}\right) \right] \delta(q);$$

$$q = \frac{\omega}{v} - \sqrt{\omega^2 - \mathbf{K}_\perp^2} + \tau_z - \frac{\omega}{2} (\text{Re } g_0 - \theta_s^2);$$

$$\theta_s = \frac{E_s}{E} \sqrt{\frac{L}{L_R}}.$$

Here g_τ, g_0 are the Fourier components of the crystal dielectric constant. These values are directly connected with the coherent scattering amplitude of the photons by the atoms of the crystal [1, 7]; θ_s is the angle of multiple scattering; $E_s \simeq 21$ MeV and L_R is the radiation length [6].

Formula (3) is written in the coordinate system with the z -axis directed along the particle velocity \mathbf{v} ; $\mathbf{K}_\perp = \omega \mathbf{n}_\perp$; and $L_a = (\omega \text{Im } g_0)^{-1}$ is the absorption length of the crystal for X-rays of frequency ω .

The analysis of formula (3) shows that the PX angular distribution consists of a series of peaks (reflections) which are located along the diffraction directions defined by the vectors

$$\mathbf{K}_B = \omega_B \mathbf{v} + \boldsymbol{\tau}; \quad \widehat{\mathbf{K}_B \mathbf{v}} = 2 \theta_B. \quad (4)$$

These vectors coincide with the directions of diffraction of the real photons with the frequency ω_B which penetrate into the crystal with an angle θ_B relative to the crystallographic planes defined by the vector $\boldsymbol{\tau}$. The frequency of PX photons in each reflection is concentrated near its own frequency ω_B , which is

$$\omega_B = \frac{\tau^2}{2 |\tau_z|} = \frac{\tau}{2 \sin \theta_B}. \quad (5)$$

Thus, the distribution of PX reflections depends on the crystal structure and on the angles between \mathbf{v} and the crystallographic planes, but is not related to the particle energy. The intensity of PX is proportional to $|g_\tau|^2$ and therefore it is largest in those crystals where the density of atoms is maximum. This condition is fulfilled in crystals with lattices of the diamond type. Figure 1 shows the distribution of the most intense reflections of PX for three mutually perpendicular directions of the particle incidence in such crystals. The values of angles and frequencies corresponding to photons in these reflections are listed in table I. These numerical data can be also used for arbitrary crystal orientation because a rotation of the crystal of an angle $\Delta\theta$ in some direction leads to a rotation of PX reflections of an angle $2 \Delta\theta$ in the same direction and the frequency of photons in each reflection changes in accordance with formula (5).

Table Ia. — Numerical values of the parameters which define the intensity and angular distribution of the parametric X-rays from electrons in crystals having a lattice of the diamond type; the vector \mathbf{v} is directed along axis $\langle 100 \rangle$; $\theta_D = 10^{-2}$; $L \gg L_a$.

Crystal	(h, k, l)	θ_B	ω_B keV	$N_0 \times 10^6$ quanta/elect.	$\theta_{ph} \times 10^4$ $E = 50$ MeV	$\theta_{ph} \times 10^5$ $E = 900$ MeV	N_D $E = 50$ MeV	N_D $E = 900$ MeV	E_{opt} MeV
Si			12.60	0.61	5.81	0.77	1.9(- 8)	2.7(- 6)	200
Ge	{ 113 }	17.55°	12.19	0.17	2.02	1.41	3.1(- 8)	5.3(- 7)	133
C			19.14	2.31	77.0	2.74	5.1(- 10)	1.3(- 5)	244
Si	{ 111 }	35.02°	3.44	0.36	1.95	8.32	4.7(- 8)	1.6(- 6)	54
Ge			3.30	0.93	3.12	19.1	5.6(- 8)	1.3(- 6)	36
C			5.22	3.12	3.77	5.78	1.3(- 7)	9.1(- 7)	67
Si	{ 220 }	45°	4.58	0.29	1.72	4.70	4.1(- 8)	1.1(- 7)	73
Ge			4.39	0.75	2.55	11.0	5.8(- 8)	2.0(- 7)	48
C			6.96	1.62	6.92	3.27	2.2(- 8)	1.7(- 6)	90

Table Ib. — *The same for axis < 110 >.*

Crystal	(h, k, l)	θ_B	ω_B keV	$N_0 \times 10^6$ quanta/elect.	$\theta_{ph} \times 10^4$ $E=50$ MeV	$\theta_{ph} \times 10^5$ $E=900$ MeV	N_D $E=50$ MeV	N_D $E=900$ MeV	E_{opt} MeV
Si	{ 113 }	25.24°	8.90	0.35	2.84	1.73	3.1(- 8)	7.7(- 7)	144
Ge			8.53	0.83	4.03	2.92	4.2(- 8)	1.3(- 6)	95
C			13.6	1.71	36.6	1.91	3.9(- 10)	4.2(- 6)	173
Si	{ 220 }	30°	6.48	0.57	1.91	2.54	8.5(- 8)	9.0(- 7)	104
Ge			6.21	1.35	2.65	5.33	1.2(- 7)	1.1(- 6)	68
C			9.85	3.22	16.4	2.14	4.3(- 9)	5.8(- 6)	125
Si	{ 400 }	45°	6.48	0.19	1.91	2.54	4.9(- 8)	5.2(- 7)	104
Ge			6.21	0.47	2.65	5.33	7.3(- 8)	7.4(- 7)	68
C			9.85	0.91	16.4	2.14	2.7(- 9)	3.5(- 6)	125

Table Ic. — *The same for axis < 111 >.*

Crystal	(h, k, l)	θ_B	ω_B keV	$N_0 \times 10^6$ quanta/elect.	$\theta_{ph} \times 10^4$ $E=50$ MeV	$\theta_{ph} \times 10^5$ $E=900$ MeV	N_D $E=50$ MeV	N_D $E=900$ MeV	E_{opt} MeV
Si	{ 113 }	10.03°	21.81	1.74	24.3	0.93	4.2(- 9)	7.4(- 6)	345
Ge			20.93	0.46	5.1	0.59	2.0(- 8)	2.5(- 6)	233
C			33.17	3.52	199	6.31	1.2(- 10)	3.3(- 6)	423
Si	{ 111 }	19.47°	5.94	0.90	1.82	2.83	1.9(- 7)	1.7(- 6)	95
Ge			5.71	2.23	2.50	6.21	2.8(- 7)	1.9(- 6)	64
C			9.02	9.78	13.3	2.35	6.4(- 8)	2.2(- 5)	115
Si	{ 113 }	31.48°	7.28	0.21	2.13	1.92	2.7(- 8)	4.0(- 7)	115
Ge			6.98	0.51	2.94	4.24	3.8(- 8)	5.1(- 7)	78
C			11.06	1.20	23.2	1.90	2.0(- 9)	2.2(- 6)	48
Si	{ 400 }	35.27°	7.93	0.28	2.34	1.58	2.7(- 8)	5.2(- 7)	125
Ge			7.61	0.65	3.27	3.51	3.7(- 8)	6.8(- 7)	85
C			12.07	1.38	30.0	1.87	1.3(- 10)	2.3(- 6)	158

3. Let us now consider the spectral and angular distributions of PX intensity within a definite reflection. For example, if one detects the angular distribution only, the integration over ω can be fulfilled in formula (3) and the result is

$$\frac{\partial^2 N}{\partial \theta_x \partial \theta_y} = \sum_{n=0}^{\infty} \frac{e^2}{4 \pi} \omega_B^{(n)} L_a \left[1 - \exp\left(-\frac{L}{L_a}\right) \right] \frac{|g_r(\omega_B^{(n)})|^2}{\sin^2 \theta_B} \cdot \frac{[\theta_x^2 \cos^2 2\theta_B + \theta_y^2]}{[\theta_x^2 + \theta_y^2 + \theta_{ph}^2]^2},$$

$$\theta_{x,y} = \frac{(\mathbf{\kappa} - \mathbf{\kappa}_B)_{x,y}}{\omega_B}; \quad \omega_B^{(n)} = \frac{\pi n}{d \sin \theta_B}; \quad \mathbf{n}_y \parallel [\mathbf{v} \tau]; \quad \mathbf{n}_x \parallel [\mathbf{n}_y \mathbf{\kappa}_B]; \quad (6)$$

$$\theta_{ph}^2 = \frac{m^2}{E^2} + \theta_s^2 - \text{Re } g_0,$$

where d is the distance between the crystallographic planes corresponding to the vector τ . It is convenient to transform expression (6) into a dimensionless form by means of the normalized amplitude $\mathfrak{J} = N/N_0$ and

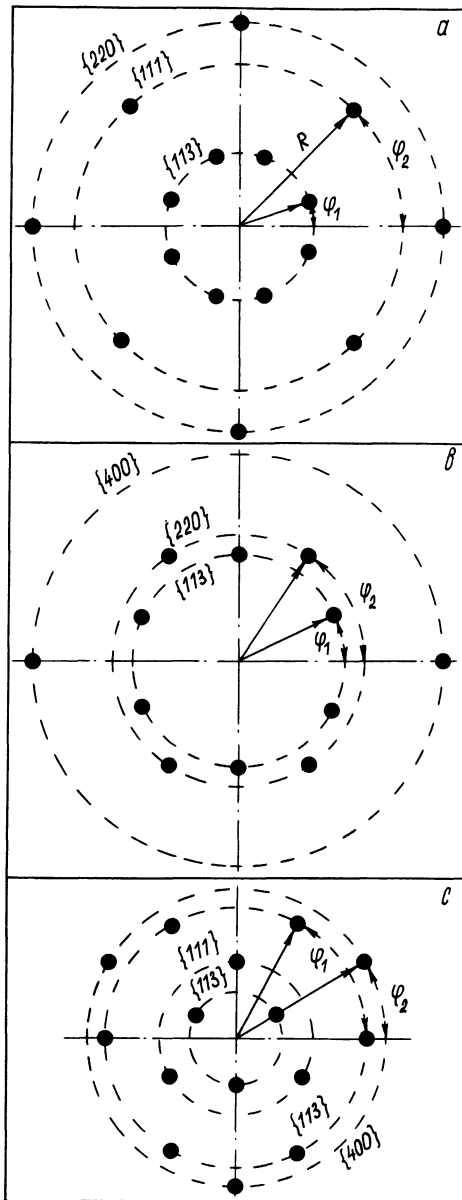


Fig. 1. — The distribution of the most intensity reflexes of the parametric X-rays in the crystals with lattice of diamond type; $R \sim \theta_B$: a) the particle velocity is directed along the axis $\langle 100 \rangle$; $\varphi_1 = 18.43^\circ$; $\varphi_2 = 45.53^\circ$; b) the same for axis $\langle 110 \rangle$; $\varphi_1 = 19.5^\circ$; $\varphi_2 = 64.3^\circ$; c) the same for axis $\langle 111 \rangle$; $\varphi_1 = 60^\circ$; $\varphi_2 = 30^\circ$.

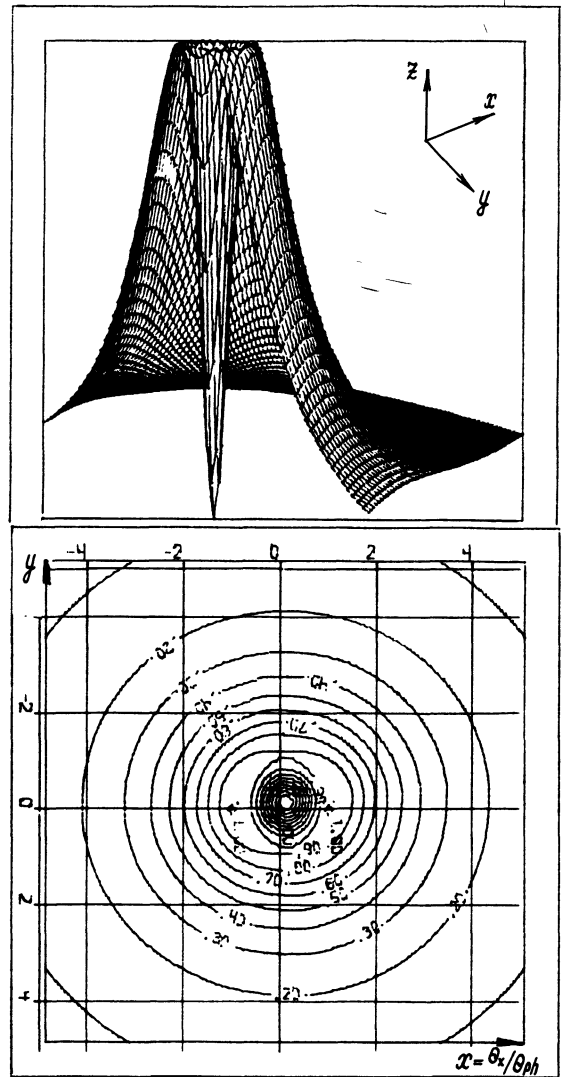


Fig. 2a. — The universal angular distribution and the lines of the uniform intensity of the radiation in the PX reflexes; x-axis is in the plane of the vectors \mathbf{v} and $\boldsymbol{\tau}$; y-axis is perpendicular to this plane; z-axis is directed along the vector $\boldsymbol{\kappa}_B$; $\theta_B = 9^\circ$.

angles $x, y = \theta_{x,y}/\theta_{ph}$:

$$\frac{\partial^2 N}{\partial x \partial y} = N_0 \mathcal{J}(x, y); \quad \mathcal{J}(x, y) = \frac{x^2 \cos^2 2\theta_B + y^2}{(x^2 + y^2 + 1)^2}; \tag{7}$$

$$N_0 = \sum_{n=0}^{\infty} \frac{e^2}{4\pi} \omega_B^{(n)} L_a \left[1 - \exp\left(-\frac{L}{L_a}\right) \right] \frac{|g_{\tau}(\omega_B^{(n)})|^2}{\sin^2 \theta_B}.$$

Then the function $\mathcal{J}(x, y)$ is the same for different crystals and figure 2 shows its typical form for several reflec-

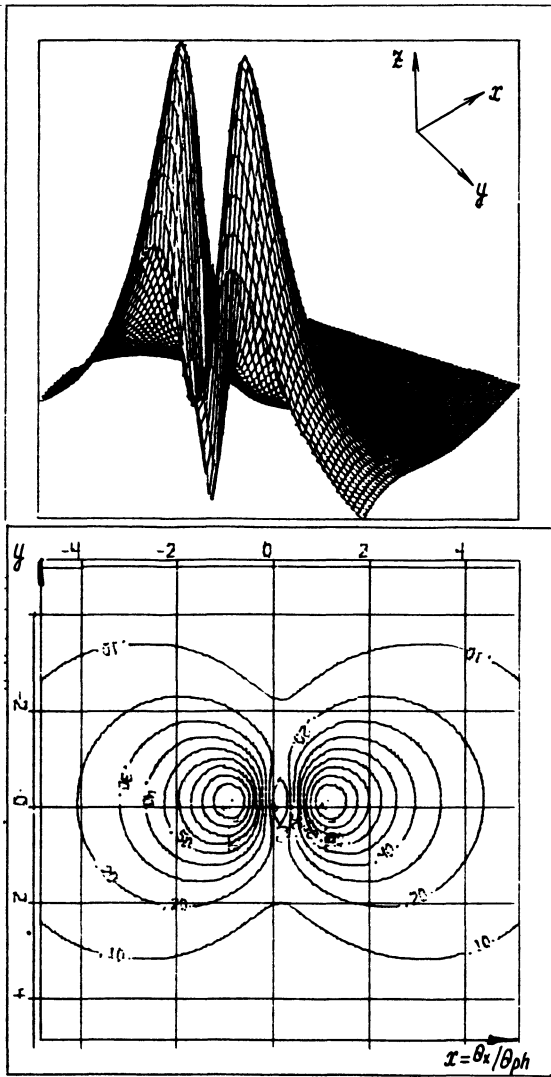


Fig. 2b. — The same for $\theta_B = 30^\circ$.

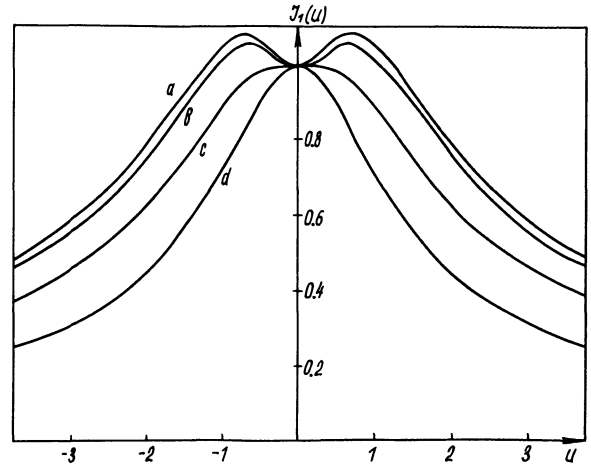


Fig. 3. — The universal spectral distribution of the radiation in the PX reflexes : a) $\theta_B = 5^\circ$; b) $\theta_B = 15^\circ$; c) $\theta_B = 30^\circ$; d) $\theta_B = 45^\circ$; the minimum for $u = 0$ is appeared when $\theta_B < \pi/8$.

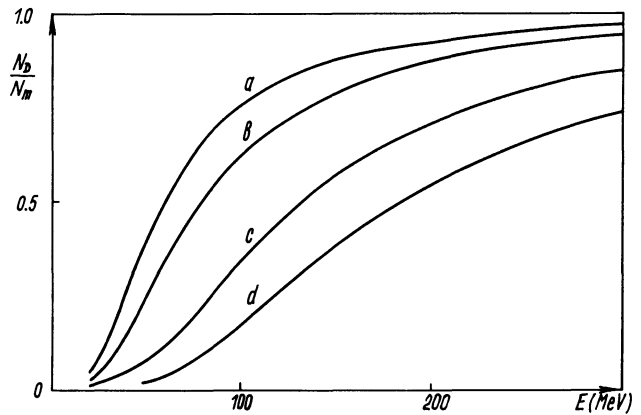


Fig. 4. — The number of photons N_D , got into the detector with angular size θ_D as a function of the particle energy; $N_m = \lim_{\theta_D \rightarrow \infty} N_D$; a) C; { 131 }; $\theta_D = 10^{-2}$; $L = L_a$; b) C; { 111 }; $\theta_D = 10^{-2}$; $L = 0.1 L_a$; c) C; { 111 }; $\theta_D = 10^{-2}$; $L = L_a$; d) C; { 111 }; $\theta_D = 10^{-3}$; $L = L_a$.

tions. Table I also lists the parameters N_0 and θ_{ph} which define the absolute values of the intensity and characteristic angular spread for the reflection.

One can find an analogous form for the frequency distribution within the PX reflection which is obtained by integrating over \mathbf{n}_\perp in formula (3)

$$\frac{\partial N}{\partial u} = N_1 J_1(u);$$

$$J_1(u) = \frac{1 + u^2(1 + \cos^2 2\theta_B)}{[1 + u^2]^{3/2}}, \tag{8}$$

where

$$N_1 = \frac{\pi}{2} N_0; \quad u = \frac{\sin \theta_B}{\cos \theta_B} \frac{(\omega - \omega_B)}{\omega_B \theta_{ph}}.$$

This universal function is shown in figure 3.

PX angular and spectral distributions have the same form for different crystals because this radiation is generated by a charged particle moving with an uniform velocity. As a result PX characteristics do not depend on the interaction between the particle and the atoms of the crystal.

The total number of photons recorded by a detector of angular size θ_D is defined by the following expression

$$N_D = \pi N_0 (1 + \cos^2 2\theta_B) \int_0^{\rho_D} \frac{\rho^3 d\rho}{(\rho^2 + 1)^2} = N_1 (1 + \cos^2 2\theta_B) \left\{ \ln \frac{\theta_D^2 + \theta_{ph}^2}{\theta_{ph}^2} - \frac{\theta_D^2}{\theta_D^2 + \theta_{ph}^2} \right\}, \quad (9)$$

where $\rho_D = \frac{\theta_D}{\theta_{ph}}$.

The value N_D depends on the detector angular size even for $\theta_D \gg \theta_{ph}$ as distinct from bremsstrahlung and channelling radiation. This circumstance is conditioned by the slow decrease $\sim \theta^{-1}$ of the PX intensity.

According to formula (9) the PX intensity has no marked threshold character. But its angular distribution is defined by the parameter $\theta_{ph} = \theta_{ph}(E)$ which increases for the electron energy

$$E < E_{opt} = \sqrt{\frac{m^2 + E_s^2 \frac{L}{L_R}}{|\operatorname{Re} g_0|}} \quad (10)$$

in accordance with formula (6). The values E_{opt} for different crystals are listed in table I.

As a result, the number of photons recorded by the

detector decreases quickly for $E < E_{opt}$. In this case formula (9) transforms as follows

$$N_D \simeq N_1 (1 + \cos^2 2\theta_B) \frac{1}{2} \left(\frac{\theta_D}{\theta_{ph}} \right)^4 \sim \left(\frac{E}{E_{opt}} \right)^4, \\ E \ll E_{opt}.$$

Figure 4 shows the number of photons N_D as a function of E for several values θ_D and L .

We hope that the numerical calculations of the PX characteristics, carried out in our work, will be useful for the experimental investigation of this phenomenon.

Acknowledgments.

We are very grateful to Prof. V. G. Baryshevsky for stimulating discussions and continuing interest in our work. We are also grateful to V. F. Zharkov for his help in the numerical calculations.

References

- [1] BARYSHEVSKY, V. G., FERANCHUK, I. D., *J. Physique* **44** (1983) 913.
- [2] BARYSHEVSKY, V. G., FERANCHUK, I. D., *Nucl. Instrum. Methods* **228** (1985) 490.
- [3] ZRELOV, Y. P., VAVILOV-CHERENKOV, *Radiation and its application in the high energy physics* (Moscow Atomizdat) 1968.
- [4] LANDAU, L. D., LIFSHITZ, E. M., *Electrodynamics of the continuous media* (Moscow Gostehizdat) 1959.
- [5] FERANCHUK, I. D., *Crystallographija* **24** (1979) 289.
- [6] TER-MIKAEIJAN, M. L., *High energy electromagnetic processes in condensed medium*, Interscience tracts on Physics and Astronomy (J. Wiley) 1972, No 29.
- [7] BATTERMAN, B., COLE, H., *Rev. Mod. Phys.* **36** (1964) 681.